Reaction Pathway to the Synthesis of Anatase via the Chemical Modification of Titanium Isopropoxide with Acetic Acid

R. Parra,*,† M. S. Góes,† M. S. Castro,‡ E. Longo,† P. R. Bueno,† and J. A. Varela†

Departamento de Físico-Química, Instituto de Química de Araraquara, São Paulo State University−UNESP, Rua Prof. Francisco Degni s/n, 14800-900 Araraquara SP, Brazil, and Instituto de Investigaciones en Ciencia y Tecnología de Materiales (INTEMA, UNMdP−CONICET), J.B. Justo 4302, B7608FDQ Mar del Plata, Argentina

Received August 13, 2007. Revised Manuscript Received October 3, 2007

Anatase nanoparticles were obtained through a modified sol–gel route from titanium isopropoxide modified with acetic acid in order to control hydrolysis and condensation reactions. The modification of $Ti(O^iPr)_4$ with acetic acid reduces the availability of groups that hydrolyze and condense easily through the formation of a stable complex whose structure was determined to be $Ti(OCOCH_3)(O^iPr)_2$ by means of FTIR and ^{13}C NMR. The presence of this complex was confirmed with FTIR in the early stages of the process. A doublet in 1542 and 1440 cm^{-1} stands for the asymmetric and symmetric stretching vibrations of the carboxylic group coordinated to Ti as a bidentate ligand. The gap of 102 cm^{-1} between these signals suggests that acetate acts preferentially as a bidentate rather than as a bridging ligand between two titanium atoms. The use of acetic acid as modifier allows the control of both the degree of condensation and oligomerization of the precursor and leads to the preferential crystallization of TiO_2 in the anatase phase. A possible reaction pathway toward the formation of anatase is proposed on the basis of the intermediate species present in a 1:1 $Ti(O^iPr)_4$:CH_3COOH molar system in which esterification reactions that introduce H_2O into the reaction mixture were seen to be negligible. The Rietveld refinement and TEM analysis revealed that the powder is composed of isotropic anatase nanocrystallites.

Introduction

Titanium dioxide (TiO_2) has been the subject of a great deal of research during the last decades because of its outstanding physicochemical properties and the increasing demand for devices with enhanced properties with strong emphasis on environmental applications. Current interest is focused on the use of nanocrystalline TiO_2 for the development of dye-sensitized solar cells (DSSCs),[1–4] photocatalysts for the degradation of water and air pollutants,[5] self-cleaning and energy efficient windows,[6] gas sensors,[7] and photoluminescent materials.[8,9] The properties of TiO_2 are significantly dependent on the crystalline phase, i.e., anatase, rutile, or brookite.[10] Phase and morphology are critical parameters in determining the suitability of the material for a particular application. Among the different TiO_2 polymorphs, anatase is a metastable phase with the highest condensation of octahedra (four shared edges per octahedron) but the lowest density. The consequent strong repulsion of the titanium cations across the shared edges is accommodated by shortening of the four shared edges and a corresponding lengthening of the four unshared edges, leading to strongly elongated octahedra in the direction of the *c*-axis and a shortening of the distances normal to this *c*-axis.[11]

Because of its high photoactivity, anatase is the most favorable phase for solar energy conversion and photocatalysis.[12,13] However, some powder processing techniques usually lead to anatase accompanied by traces of rutile or brookite.[13,14] Numerous efforts have been made toward the synthesis of high surface area anatase from different precursors ($Ti(O^nBu)_4$, $Ti(O^iPr)_4$, $TiCl_4$, $TiCl_3$, $Ti(SO_4)_2$) and by different synthesis routes such as hydrothermal, thermohydrolysis, and sol–gel processes.[14–17] Among the proven chemical methods of

* To whom correspondence should be addressed. E-mail: rparra@fi.mdp.edu.ar (R.P.); varela@iq.unesp.br (J.A.V.). Tel: 55 16 33016642. Fax: 55 16 33227932.
† Departamento de Físico-Química.
‡ Instituto de Investigaciones en Ciencia y Tecnología de Materiales.

(1) Vlachopoulos, N.; Liska, P.; Augustynski, J.; Gräetzel, M. *J. Am. Ceram. Soc.* **1988**, *110*, 1216–1220.
(2) O'Regan, B.; Grätzel, M. *Nature* **1991**, *353*, 737–740.
(3) Nazeeruddin, M. K.; Kay, A.; Rodicio, L.; Humpbry-Baker, R.; Mueller, E.; Liska, P.; Vlachopoulos, N.; Grätzel, M. *J. Am. Ceram. Soc.* **1993**, *115*, 6382–6390.
(4) Barbé, C. J.; Arendse, F.; Comte, P.; Jirousek, M.; Lenzmann, F.; Shklover, V.; Grätzel, M. *J. Am. Ceram. Soc.* **1997**, *80*, 3157–3171.
(5) Choi, H.; Kim, Y. J.; Varma, R. S.; Dionysiou, D. D. *Chem. Mater.* **2006**, *18*, 5377–5384.
(6) Werner, A.; Roos, A. *Sol. Energy Mater. Sol. Cells* **2007**, *91*, 609–615.
(7) Kim, I. D.; Rothschild, A.; Lee, B. H.; Kim, D. Y.; Jo, S. M.; Tuller, H. L. *Nano Lett.* **2006**, *6*, 2009–2013.
(8) Liu, Y.; Claus, R. O. *J. Am. Chem. Soc.* **1997**, *119*, 5273–5274.
(9) Abazovic, N. D.; Comor, M. I.; Dramicanin, M. D.; Jovanovic, D. J.; Ahrenkiel, S. P.; Nedeljkovic, J. M. *J. Phys. Chem. B* **2006**, *110*, 25366–25370.
(10) Barnard, A. S.; Curtiss, L. A. *Nano Lett.* **2005**, *5*, 1261–1266.
(11) Grey, I. E.; Wilson, N. C. *J. Solid State Chem.* **2007**, *180*, 670–678.
(12) Khanna, P. K.; Singh, N.; Charan, S. *Mater. Lett.* **2007**, *25*, 4725–4730.
(13) Hsiao, P.-T.; Wang, K.-P.; Cheng, C.-W.; Teng, H. *J. Photochem. Photobiol., A* **2007**, *188*, 19–24.
(14) Zhang, H.; Finnegan, M.; Banfield, J. F. *Nano Lett.* **2001**, *1*, 81–85.
(15) Pillai, S. C.; Periyat, P.; George, R.; McCormack, D. E.; Seery, M. K.; Hayden, H.; Colreavy, J.; Corr, D.; Hinder, S. J. *J. Phys. Chem. C* **2007**, *111*, 1605–1611.
(16) Li, J. G.; Ishigaki, T.; Sun, X. *J. Phys. Chem. C* **2007**, *111*, 4969–4976.

10.1021/cm702286e CCC: $40.75
Published on Web 11/20/2007

synthesis for high-purity inorganic nanostructured materials, the sol–gel is an advantageous and reproducible one. It leads to nanoparticles, high surface areas and meso to macroporous materials. Furthermore, given the reactivity and versatility of the chemicals used in the alkoxide-based sol–gel route, it is possible to work at low temperatures and obtain materials in metastable phases otherwise unattainable.[18]

To synthesize pure anatase TiO_2 powders with a homogeneous nanosized particle distribution, the experimental conditions (pH, *T*, Ti:H_2O ratio, the use of modifiers and/or surfactants) must be under control. It has been established that strong acids and high temperatures promote the protonation of Ti−O−Ti bridges and activate redissolution−precipitation reactions that ultimately lead to rutile. In contrast, in mild acidic media and low temperatures, the solid precipitates into small particles that are almost insoluble in the liquid; therefore, Ostwald ripening is negligible and anatase, the precipitated phase, preserved.[19]

Although they are successfully used, commercial TiO_2 powders are generally produced by a pyrolysis route from $TiCl_4$ and are a mixture of 70% anatase and 30% rutile, aproximately.[20] In addition, when titanium chloride is used as precursor or HCl as catalyst for hydrolysis, the surface of the resulting TiO_2 nanoparticles is inevitably contaminated with chlorine ions. To the best of our knowledge, the influence of such species on the performance of solar cells, photocatalysts, or gas sensors has not yet been reported in the literature. Almeida et al. have reported the synthesis of TiO_2 in 0.1 M nitric acid, which yielded a mixture of anatase and brookite.[21] Under similar conditions, Hsiao et al. reported that the TiO_2 synthesized by a conventional sol–gel route consisted in anatase with small quantities of the two other polymorphs[13] and Hart et al. achieved the crystallization of anatase with small amounts of brookite after an aging period at 95 °C.[22] On the other hand, Pillai et al. have recently shown that anatase can be retained up to 97% after an 800 °C treatment by modifying the Ti(O^iPr)$_4$ precursor with urea.[15] Wang and co-workers reported on the hydrothermal synthesis of the TiO_2 polymorphs. During the synthesis in ethanol via the stabilization of $TiCl_4$ with acetic acid, the authors observed that the release of a large amount of HCl attributable to the reaction between $TiCl_4$ and H_2O hinders the chelation of Ti(IV) with acetate, because it exists mainly as acetic acid. Under those experimental conditions, acetic acid would not have a stabilizing effect and the released HCl catalyzes the hydrolysis reactions that finally lead to rutile.[17] As well, Li et al. showed that anatase, rutile, and especially brookite could be selectively synthesized via redox reactions under mild hydrothermal conditions with $TiCl_3$ as precursor for TiO_2.[16]

In the present paper, we report on the phase formation and on the structural and morphological features of pure anatase obtained by a modified sol–gel method via the chemical modification of titanium isopropoxide with glacial acetic acid. The main goal of this work is to identify the species present throughout the synthesis process and contribute to the understanding of the mechanism of anatase synthesis.

Experimental Section

Analytical-grade reagents were used as supplied without further purification. Titanium isopropoxide (62 mmol, Ti(O^iPr)$_4$, Aldrich, 97%) was added at room temperature to 10 mL of 2-propanol (Pr^iOH) along with anhydrous acetic acid (CH_3COOH, Merck), in a 1:1 Ti: CH_3COOH molar ratio, in order to control the condensation reactions. The solution was stirred for 60 min, after which a diluted aqueous solution of nitric acid (HNO_3, Qhemis, 65%) prepared as to achieve a final pH value between 5 and 6 and a 1.33 Ti:H_2O ratio, was added dropwise. The colloidal dispersion was put into a Petri dish and stored for 50 h inside a desiccator at room temperature for solvent evaporation. The obtained white cake was crushed into powder in an agate mortar, washed with distilled water and calcined in an electric furnace at several temperatures with a heating rate of 5 °C/min. No surfactants were used in this synthesis route.

The X-ray diffraction data (XRD) were collected using a Rigaku RINT2000 rotating anode diffractometer (42 kV, 120 mA) with Cu k_α radiation ($\lambda_{k_{\alpha1}} = 1.5405$ Å, $\lambda_{k_{\alpha2}} = 1.5443$ Å, $I_{k_{\alpha1}}/I_{k\alpha2} = 0.5$) monochromatized by a curved graphite crystal. An interval from 20° to 130° 2θ, with a step size of 0.02° (2θ), 3.5 s per step, and divergence and receiving slits of 0.5 and 0.3 mm, respectively, were the selected conditions for Rietveld refinement.[23] The refinements were calculated using the program package General Structure Analysis System (GSAS)[24] suite with EXPGUI[25] interface. The peak profile function was modeled using a convolution of the Thompson−Cox−Hastings pseudo-Voigt (pV-TCH)[26] with an asymmetry function that accounts for the asymmetry due to axial divergence according to the methodology described by Finger et al.[27] To account for the anisotropy in the half-width of the reflections, the bidimensional model for crystallite size described by Larson and Von Dreele[24] was applied. The model described by Stephens[28] was used for the anisotropic strain. A CeO_2 (Acros organics, 99.9%) powdered sample heated at 1530 °C for 4 h was used as the crystalline standard, representing instrumental broadening, with the same profile function used for the TiO_2 sample.

The following parameters were refined: atomic coordinates, occupancies, unit cell, scale factor, sample displacement, atomic displacement, and full width at half-maximum (fwhm), which can be correlated with crystallite size and microstrain. As an aid to the eye, a simulation of the theoretical X-ray powder pattern of a possible TiO_2 sample was carried out with the GSAS[24] on the basis of the ICDD-PDF according to the files 84–1285, 76–1934, and 78–2485 for anatase (21%), brookite (66%), and rutile (13%), respectively. The percentage of each allotropic phase was selected in order to attain a well-resolved pattern.

(17) Wang, C.; Deng, Z. X.; Li, Y. *Inorg. Chem.* **2001**, *40*, 5210–5214.
(18) Tang, J.; Redl, F.; Zhu, Y.; Siegrist, T.; Brus, L. E.; Steigerwald, M. L. *Nano Lett.* **2005**, *5*, 543–548.
(19) Jolivet, J.-P. *De la solution à l'oxyde: Condensation des cations en solution aqueuse. Chimie de surface des oxydes*; InterEdition/CNRS: Paris, 1994.
(20) Grätzel, M. *J. Sol−Gel Sci. Technol.* **2001**, *22*, 7–13.
(21) de Almeida, P.; van Deelen, J.; Catry, C.; Sneyers, H.; Pataki, T.; Andriessen, R.; Van Roost, C.; Kroon, J. M. *Appl. Phys. A: Mater. Sci. Process.* **2004**, *79*, 1819–1828.
(22) Hart, J. N.; Bourgeois, L.; Cervini, R.; Cheng, Y.-B.; Simon, G. P.; Spiccia, L. *J. Sol-Gel Sci. Technol.* **2007**, *42*, 107–117.
(23) Rietveld, H. *J. Appl. Crystallogr.* **1969**, *2*, 65–71.
(24) Larson, A. C.; Von Dreele, R. B. *GSAS: General Structure Analysis System*. Report LAUR 86–748; Los Alamos National Laboratory:Los Alamos, NM, 2004.
(25) Toby, B. H. *J. Appl. Crystallogr.* **2001**, *34*, 210–213.
(26) Young, R. A.; Desai, P. *Arch. Nauki Mater.* **1989**, *10*, 71–90.
(27) Finger, L. W.; Cox, D. E.; Jephcoat, A. P. *J. Appl. Crystallogr.* **1994**, *27*, 892–900.
(28) Stephens, P. *J. Appl. Crystallogr.* **1999**, *32*, 281–289.

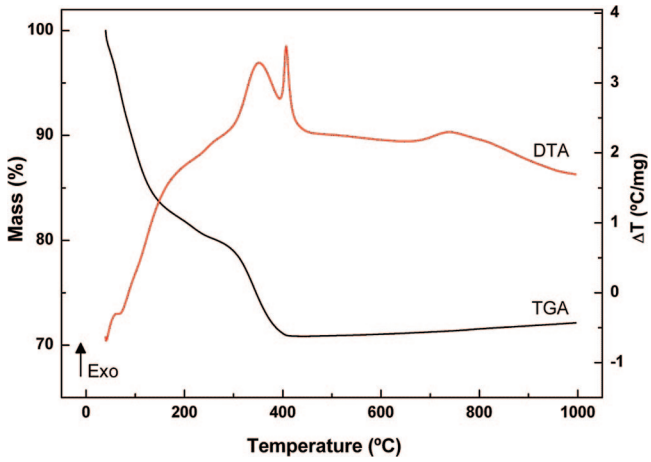

Figure 1. Thermal behavior of the synthesized powder.

For high-resolution transmission electron microscopy (HR-TEM, Philips CM200), the powder was dispersed in ethanol in an ultrasonic bath and deposited by dipping onto carbon-coated copper grids. Thermogravimetric and differential thermal analyses (TGA/DTA) were performed with a simultaneous module, SDT Q600 (TA Instruments), under a dynamic atmosphere of synthetic air (50 mL/min) with a heating rate of 10 °C/min up to 1000 °C. Raman spectra were registered with a Bruker RFS 100/S spectrometer equipped with a Nd:YAG laser (1064 nm; 250 mW) as excitation source and, for band gap determination, UV–vis reflectance spectra were acquired with a Cary 5G spectrometer in the 300−800 nm range. Infrared spectra measurements were carried out by means of a Nicolet Impact 400 spectrometer in the 4000–400 cm^{-1} wavenumber range using KBr pellets.

^{13}C NMR spectra were acquired with a Varian Innova UNIY-300 spectrometer using a 7 mm MAS NMR probe. Measurements were carried out with the static probe at 75.4 MHz, using 90° pulses of 5.2 μs and a recycle delay of 25 s, and eventually, in the absence of solvent (2-propanol) in order to avoid inconveniently large signals that mask the resonances of interest. Chemical shifts are reported relative to TMS. The system Ti(O^{i}Pr)$_4$:CH$_3$COOH, with ratios ranging from 1:1 to 1:6, was studied as well as reference samples of the reactants alone and mixtures Ti(O^{i}Pr)$_4$ + Pr^{i}OH, CH$_3$COOH + Pr^{i}OH, Ti(O^{i}Pr)$_4$ + CH$_3$COOH + Pr^{i}OH and Ti(O^{i}Pr)$_4$ + CH$_3$COOH + Pr^{i}OH + H$_2$O. Samples were prepared 60 min before being analyzed.

Results

Figure 1 shows the thermal behavior of the synthesized powder previously reserved at 50 °C for 72 h. The TGA curve exhibits three mass losses associated with endothermic and exothermic events in the DTA curve. The first endothermic event occurring around 80 °C corresponds to the elimination of adsorbed water. The following two exothermic events at 100–250 °C (17 wt % loss) and 300–400 °C (10 wt % loss) are due to the volatilization and combustion of hydration−water and adsorbed HNO$_3$ and organic species such as Pr^{i}OH and CH$_3$COOH. The sharp peak in the DTA curve starting at 380 °C, approximately, corresponds to the crystallization of the amorphous residue into anatase, whereas that around 670 °C indicates the phase transition anatase−rutile. There are no associated signals with these latter thermal events in the TGA curve confirming the crystallization and phase transition events.

The XRD patterns in Figure 2a show the phase evolution of the synthesized powder when calcined at different temperatures where the phase transition into rutile phase is seen to start around 650 °C. The simulated pattern included in this figure leads to the hypothesis that the synthesized TiO$_2$ consists in the anatase phase only up to calcination temperatures around 650 °C.

The refined unit-cell parameters achieved by the Rietveld method of the pattern resultant from the powder treated at 450 °C for 2 h (Figure 2b) allowed us to confirm the sole presence of anatase (space group $I4_1/amd$). Final values of lattice parameters, volume, atomic positions, and density are shown in Table 1. The calculated crystallite sizes were of 41.7 nm (perpendicular *c*-axis) and 35.4 nm (parallel *c*-axis) revealed that crystallites are almost isotropic.

The morphology of the obtained powder was characterized by means of TEM. In the dark-field image of the dry gel shown in Figure 3a, crystalline nuclei of 5 nm, approximately, can be recognized within an amorphous matrix, indicating that the desired phase has already formed before the thermal treatment. Figure 3b shows that the powder treated at 450 °C for 2 h is composed of particles with sizes that range from 10 to 30 nm, which are comparable to the average crystallite size determined by the Rietveld refinement of the XRD data and it can also be observed that crystallites are isotropic. The selected area for electron diffraction pattern analysis (SAED), inset in Figure 3b, confirmed that the particles are well-crystallized in the anatase phase, in good agreement with the ICDD-PDF 84–1285 and XRD results. A lattice fringe of 3.52 Å, corresponding to the plane (101) of anatase, was measured from Figure 3c registered for this sample under HR-TEM.

The results obtained with XRD and TEM are further supported by the Raman analysis of the powder treated at 450 °C for 2 h. The spectrum shown in Figure 4 exhibits well-defined bands at 638, 515, 394, 195, and 143 cm^{-1} which are the characteristic bands for anatase.[29,30] Neither the signals of brookite (249, 323, 366, and 407 cm^{-1})[13] nor those of rutile (826, 612, 447, and 143 cm^{-1})[30] appear in the spectrum. In addition, there are no traces of organic matter. The UV–vis reflectance of the TiO$_2$ powder treated at 450 °C for 2 h (not shown) is characterized by a quick transition from absorption at the near-UV region to high reflectance at the blue edge (∼400 nm) of the visible spectrum. According to the Kubelka–Munk model,[31] a value of 3.16 eV, associated with a wavelength of 392 nm, was the estimated energy for the optical band gap of the synthesized anatase.

By means of FTIR, the formation of a Ti−acetate complex in the early stages of the process was confirmed. The spectra of the initial solution consisting of Pr^{i}OH and CH$_3$COOH (a), that of the initial solution after the addition of Ti(O^{i}Pr)$_4$ (b), and that of the dry gel after the addition of the diluted

(29) Balaji, S. Y. D. J. R. *J. Raman Spectrosc.* **2006**, *37*, 1416–1422.
(30) Bassi, A. L.; Cattaneo, D.; Russo, V.; Bottani, C. E.; Barborini, E.; Mazza, T.; Piseri, P.; Milani, P.; Ernst, F. O.; Wegner, K.; Pratsinis, S. E. *J. Appl. Phys.* **2005**, *98*, 074305–9.
(31) Jahan, F.; Islam, M. H.; Smith, B. E. *Sol. Energy Mater. Sol. Cells* **1995**, *37*, 283–293.

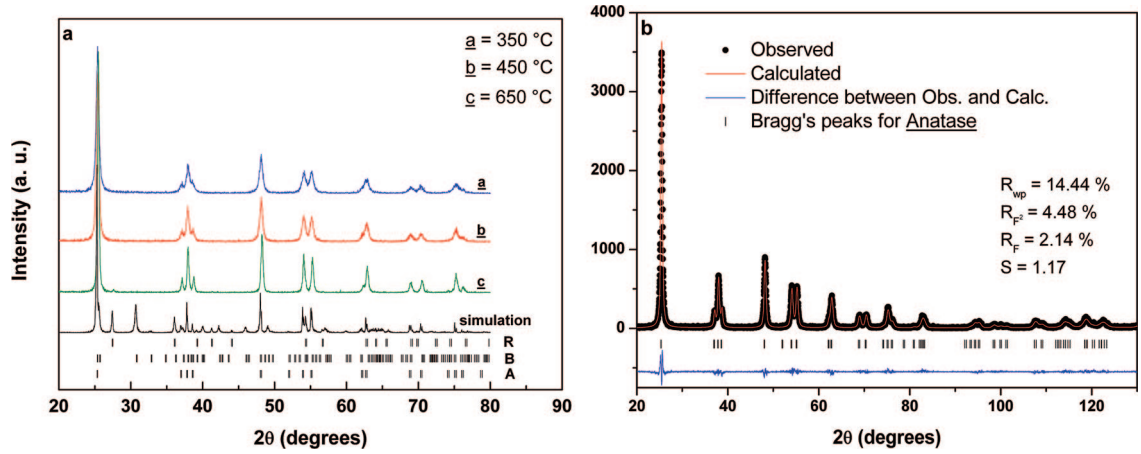

Figure 2. (a) XRD patterns registered after different calcination temperatures (R, rutile; B, brookite; and A, anatase) and (b) Rietveld plot for the powder treated at 450 °C.

Table 1. Phase Data and Atomic Parameters for Anatase Phase Calculated by Rietveld's Method

Phase Data	
space group	$I4_1/amd$
a (Å)	3.7857(1)
c (Å)	9.5056(4)
V (Å^3)	136.23(1)
d (g/cm^3)	3.895
c/a	2.5109
length Ti−O (Å)	1.9603(19) and 1.9381(4)

Atomic Parameters							
atom	charge	Wyckoff	site	x/a	y/b	z/c	U (Å^2)
Ti	+4	4b	−4m2	0	0.25	0.375	0.0030(2)
O	−2	8e	2mm	0	0.25	0.1687(2)	0.0076(6)

HNO_3 aqueous solution (c) are shown in Figure 5. The relevant features in spectrum a are the strong sharp band at 1715 cm^{-1} corresponding to the stretching vibration of the hydrogen bonded C═O group of the acetic acid, and those around 1385 and 1280 cm^{-1} due to the vibration modes of the COO group.[32] The doublet in 1542 and 1440 cm^{-1} in spectrum b stands for the asymmetric and symmetric stretching vibrations of the carboxylic group coordinated to Ti as a bidentate ligand.[33] Moreover, the separation between these signals ($\Delta\nu$ = 102 cm^{-1}) suggests that acetate acts preferentially as a bidentate rather than as a bridging ligand between two titanium atoms. According to the literature, the $\Delta\nu$ due to the latter possibility would be higher than 150 cm^{-1}.[33] The presence of the 1715 cm^{-1} (C═O) band can be attributed to the contribution of monodentate-coordinated acetates. Interestingly, after the addition of water, the intensity of this band diminishes noticeably, whereas those around 1542 and 1440 cm^{-1} increase and become sharper, implying that the complexation continues during condensation. The signal at 950 cm^{-1} in spectrum b indicates the presence of Pr^{i}OH, which is no longer visible in the dry gel (spectrum c).

The fading of the bands at 1160, 1124, and 1009 cm^{-1} (stretching Ti−O−C) together with the appearance of intense bands around 846 and 640 cm^{-1} in spectrum c indicate the hydrolysis of the alkoxide and the formation of Ti−O and Ti−O−Ti bonds during condensation, respectively.[34] The broadband from 3660 to 3000 cm^{-1}, associated with the stretching vibration modes of hydroxyl groups, became broader after the addition of H_2O, and a shoulder at 1630 cm^{-1} over the 1715 cm^{-1} signal appeared due to the O−OH bending mode. The presence of the bands due to acetate groups in the dry gel suggests that acetates might be retained as ligands, as hydrogen-bonded groups to hydroxo sites, or as adsorbed ions.

The ^{13}C NMR spectra registered for the Ti(O^{i}Pr)$_4$:CH$_3$COOH system are shown in Figure 6, and in Table 2, the observed signals are assigned to the resonating carbon of the identified species. The replacement of isopropoxy groups in Ti(O^{i}Pr)$_4$ by acetate groups is evidenced in spectrum a for the equimolar sample. Because of chelation, the resonance expected from the carboxylic C is shifted to higher δ values (178 ppm) with respect to the signal at 175 ppm observed for acetic acid in Pr^{i}OH. Furthermore, the

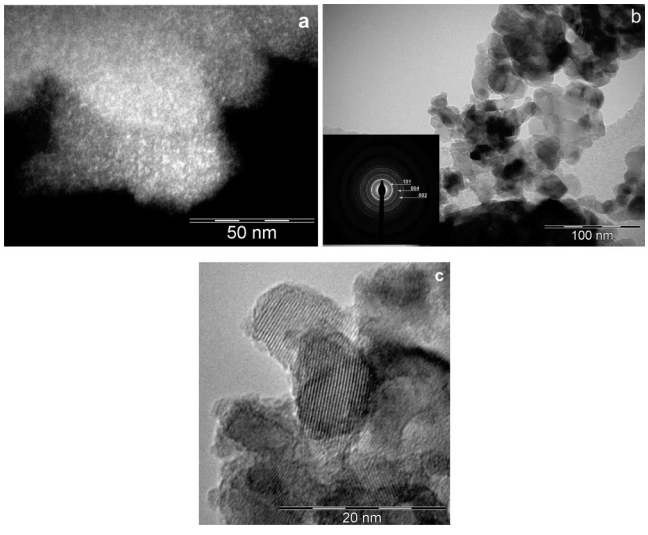

Figure 3. (a) Dark-field TEM image of the powder, (b) bright-field image and SAED pattern matching with anatase after calcination at 450 °C for 2 h, and (c) HR-TEM image showing particles oriented in the [101] direction.

(32) Socrates, G. *Infrared Characteristic Group Frequencies*, 2nd ed.; John Wiley & Sons: Sussex, U.K., 1997.
(33) Tsai, M. T. *J. Non-Cryst. Solids* **2002**, *298*, 116–130.
(34) Colomer, M.; Velasco, M.; Jurado, J. *J. Sol−Gel Sci. Technol.* **2006**, *39*, 211–222.

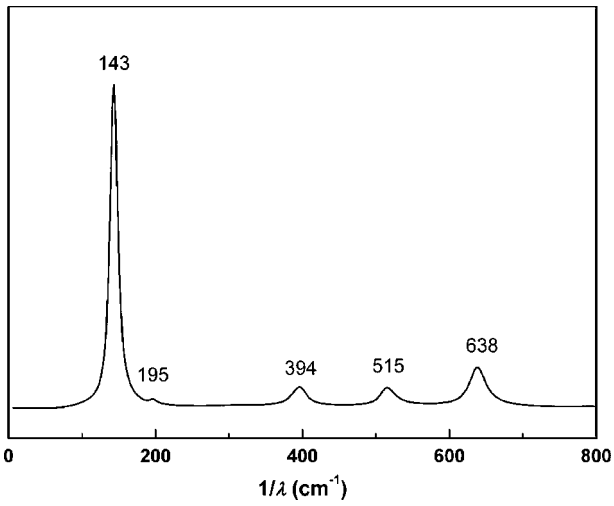

Figure 4. Raman spectrum of the powder treated at 450 °C for 2 h showing the characteristic bands of the anatase phase.

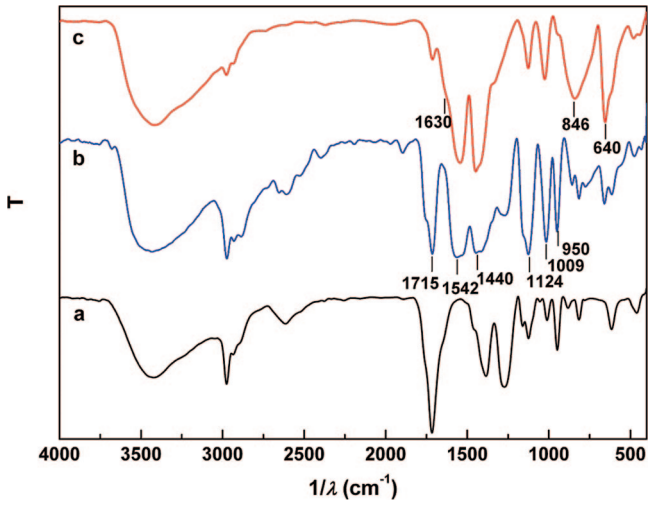

Figure 5. FTIR spectra of (a) Pr^{i}OH + CH_3COOH, (b) Pr^{i}OH + CH_3COOH + Ti(O^{i}Pr)$_4$, and (c) the dry gel obtained after the addition of a diluted HNO_3 aqueous solution.

appearance of a band around 64 ppm indicates the release of Pr^{i}OH, previously coordinated to Ti, because of the resonance of the central CH group. The resonance around 80 ppm corresponds to the CH carbon of the isopropoxy groups that remain bonded to Ti. The broadness of these resonances might be ascribed to differences in the chemical environment that surrounds the C atoms bonded to Ti such as the existence of monodentate and bidentate coordinated acetates. The signals between 21 and 26 ppm correspond to the CH_3 groups of isopropoxy and acetate groups bonded to Ti and to those of the released Pr^{i}OH.

Essential information on the reaction mechanism and on the modification of titanium isopropoxide with acetic acid is obtained after the integration of the area of the NMR signals. The integration of the signals at 64 ppm (free isopropoxy groups) and 80 ppm (isopropoxy groups coordinated to Ti) in spectrum a revealed that the 50% of the isopropoxy groups have been hydrolyzed or replaced by acetates. From the resonance of the carboxylic carbon (178 ppm), it follows that virtually all of the acetic acid has bonded to Ti. Indeed, this is in good agreement with the FTIR results

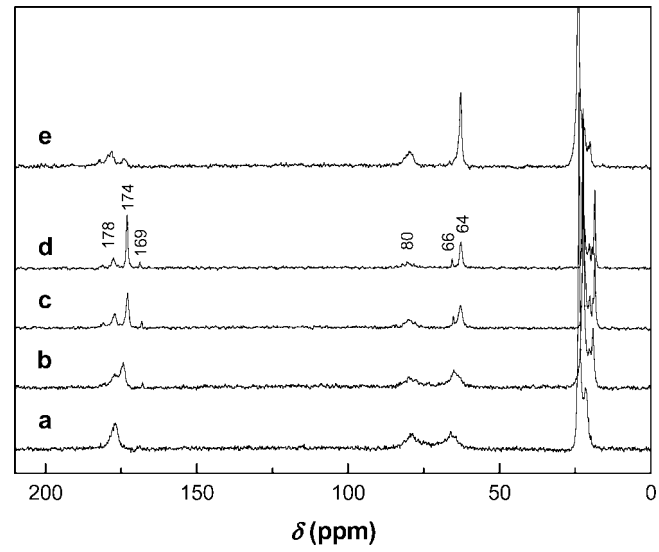

Figure 6. ^{13}C NMR spectra of different Ti(O^{i}Pr)$_4$:CH_3COOH molar ratios: (a) 1:1; (b) 1:2; (c) 1:3; (d) 1:4, and (e) 1:1 mixture after H_2O addition.

Table 2. ^{13}C NMR Peak Identification

species and resonating C (*C)	δ
Ti(OCH(*CH_3)$_2$)$_4$	26.5
Ti(O*CH(CH_3)$_2$)$_4$	79
*CH_3COOH	20.5
CH_3*COOH	174
*CH_3COO−Ti	22–24
CH_3*COO−Ti	178
(*CH_3)$_2$CHOH	25
(CH_3)$_2$*CHOH	64
*$CH_3COOCH(CH_3)_2$	21.3
CH_3COOCH(*CH_3)$_2$	21.8
CH_3COO*CH(CH_3)$_2$	66.5
CH_3*COOCH(CH_3)$_2$	169

and with a Ti(OCOCH$_3$)(O^{i}Pr)$_2$ complex structure with acetate as a bidentate ligand. Dimer structures such as Ti_2O_2(OCOCH$_3$)$_2$(O^{i}Pr)$_4$ in which acetates bridge two titanium atoms in octahedral environments, have been proposed in the literature; however, at least in the 1:1 Ti(O^{i}Pr)$_4$:CH_3COOH molar mixture before the addition of H_2O, the FTIR results disagree with this hypothesis.

Spectra b−d in Figure 6 belong to the 1:2, 1:3, and 1:4 Ti(O^{i}Pr)$_4$:CH_3COOH molar ratios, respectively. With increasing acetic acid content, the resonance due to the CH carbon in the isopropoxy groups bonded to Ti (∼80 ppm) tends to disappear, whereas that corresponding to the same group in the released Pr^{i}OH (∼64 ppm) grows in intensity. However, even with high concentrations of acetic acid, the signal of the Ti-bonded isopropoxy groups persists indicating that their complete replacement by acetates is never attained. In fact, the integration of the CH peaks indicates that the hydrolysis of the isopropoxy groups increases from 62% for the 1:2 mixture up to 67% for the 1:3 and 70% for the 1:4 and 1:6 (not shown) mixtures. For the 1:4 and 1:6 samples, respectively, it was determined that only the 33 and 30% of the acetic acid is bonded to Ti. These observations suggest that under an excess of acetic acid, the highest attainable number of chelating acetates is limited to 2 acetate groups per Ti atom. Also in Figure 6, an increase in the concentration of free acetic acid (174 ppm) can be observed in spectra

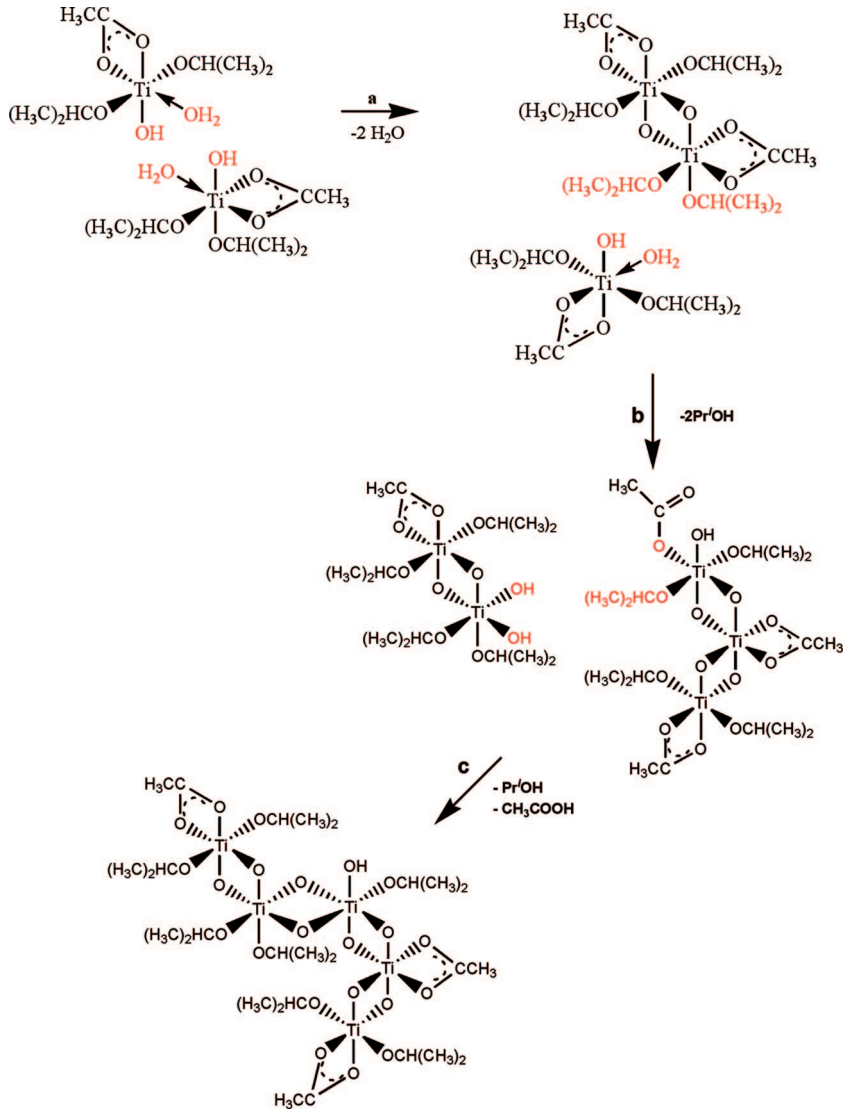

Figure 7. Possible reaction pathway leading to nanosized anatase nuclei via olation and oxolation/alkoxolation reactions.

b, c and d and, interestingly, the formation of a certain amount of isopropyl acetate is evidenced by the resonances of the COO and CH carbons of this byproduct at 169 and 66 ppm, respectively. The ester formation may occur through the condensation of Pr^{i}OH with acetic acid or through transesterification reactions between coordinated acetate or isopropoxy groups with Pr^{i}OH or acetic acid, respectively, with the simultaneous production of H_2O. The slowly release of H_2O into the solution accelerates the condensation of the precursor and makes it difficult to establish the most probable molecular structures present. As proposed in the works by Stathatos et al.[35] and Choi et al.,[36] transesterification reactions lead to direct condensation resulting in oxo/hydroxo clusters that inevitably proceed to gelation. Esterification reactions are an elegant resource to generate water in situ. However, there is no evidence of isopropyl acetate formation in the 1:1 molar mixture, and under these experimental conditions, practically all of the acetic acid is coordinated to Ti, the sol is highly stable, and gelation takes several days to occur if no water is intentionally added.

Finally, spectrum e, recorded immediately after the addition of H_2O into the 1:1 molar ratio sample, shows the rapid evolution of the hydrolysis. The peak at 64 ppm due to free Pr^{i}OH became more intense and sharper, and the release of a small quantity of acetic acid is also observed. The amount of isopropoxy groups bonded to Ti decreased from 50 to 36%, whereas 86% of the acetate remained coordinated. The powder obtained after drying the gel at 100 °C for 24 h revealed the presence of two sharp signals at 180 and 23 ppm due to the resonances of the carboxylic C of acetate coordinated or adsorbed on the surface of the TiO_2 nanoparticles.

Discussion

The synthesis and stabilization of nanocrystalline anatase as a single phase seems to be related to the partial hydrolysis of titanium isopropoxide. Under the experimental conditions here reported, in which Ti(O^{i}Pr)$_4$ reacts

(35) Stathatos, E.; Lianos, P.; Tsakiroglou, C. *Microporous Mesoporous Mater.* **2004**, *75*, 255–260.
(36) Choi, H.; Stathatos, E.; Dionysiou, D. D. *Appl. Catal., B* **2006**, *63*, 60–67.

with acetic acid turning into the less reactive species $Ti(OCOCH_3)(O^iPr)_2$, the isopropoxy groups that remain bonded to Ti can be easily hydrolyzed by the following addition of water as a nitric acid−aqueous solution. In subsequent stages of the process, the isopropoxy groups may also be removed by alkoxolation. Although it is difficult to predict an absolute structure for the zero-charge precursor of the solid phase after the addition of H_2O into the $Ti(O^iPr)_4$:CH_3COOH:Pr^iOH system, $Ti[(OH)_x(OCOCH_3)(O^iPr)_{2-x}(OH_2)_n]$, with x and n between 0 and 2, is among the most probable species present.

On the basis of the experimental results discussed above, we propose in Figure 7 a reaction pathway to the formation of anatase nanoparticles from a 1:1 $Ti(O^iPr)_4$:CH_3COOH molar mixture in which the realease of water due to esterification/transesterification reactions is minimized. After the controlled addition of H_2O, the first step leading to the condensation of the precursors involves the formation of an edge-sharing dimer between two octahedrons as shown in stage a of Figure 7. During the initial phase, condensation takes place through olation reactions due to the higher lability of water with respect to −OH, −O^{i}Pr, and monodentate and/or bidentate acetate ligands. Except H_2O, the other possible leaving groups require for acid catalysis what determines the slower rate of oxolation and alkoxolation reactions. It is the attaching of a third octahedron that determines the crystalline structure, depending on whether it locates linearly or forms a twisted chain with the dimer.[19,37] Because of the relative position in the dimer of two reacting ligands, namely $-OH_2$, −OH, or −O^{i}Pr, properly oriented for condensation, there is a higher probability for the third octahedron to attach sharing an edge in a twisted chain and thus leading to anatase. Stages b and c illustrate the possible oligomerization of the embryo that proceeds through oxolation and alkoxolation. Ultimately, a small number of acetate ligands are also hydrolyzed as detected with NMR.

The key feature of the modification of $Ti(O^iPr)_4$ with acetic acid is that it reduces the availability of groups that hydrolyze and condense easily through the formation of the $Ti(OCOCH_3)(O^iPr)_2$ complex. Therefore, the use of acetic acid as modifier allows the control of both the degree of condensation and oligomerization and leads to the preferential crystallization of TiO_2 in the anatase phase. Without the control of the condensation reactions, an amorphous mass of agglomerated particles is immediately obtained after the addition of water. That means that, with acetic acid as a bidentate ligand and under mild acidic conditions, condensation reactions advance until a point in which the nanocrystalline nuclei do not grow any further because of the unfavorable conditions for the remaining ligands to condense via alkoxolation or oxolation. Then, these small nuclei of ∼5 nm as shown in Figure 3a, are stabilized by the chosen conditions of pH, T and $Ti(O^iPr)_4$:CH_3COOH ratio. This explains how crystallization proceeds and why this synthesis methodology is capable of attaining nanocrystals of anatase phase.

In contrast, in a stronger acidic medium the hydrolysis of $Ti(O^iPr)_4$ or $Ti[(OCOCH_3)(O^iPr)_2]$ would take place to a higher extent, maybe to completion, leading to species such as $Ti[(OH)_4(OH_2)_2]$ or $Ti[(OH)_2(OCOCH_3)(OH_2)_2]$, among others. In such a situation, the probability of the dimer to grow linearly along the ecuatorial plane of the atoms into rutile would be privileged because of the great availability of well-positioned readily condensable groups through olation or acid-catalyzed oxolation.[19] Moreover, the linear accommodation of octahedrons sharing two edges would be the preferred configuration because it minimizes the interaction between the titanium atoms.

Conclusions

On the basis of FTIR and ^{13}C NMR analyses, we proposed a reaction pathway leading to the crystallization of anatase TiO_2 that involved partially hydrolyzed species. The modification of titanium isopropoxide with glacial acetic acid reduces the availability of groups that hydrolyze easily through the formation of a stable complex. The use of acetic acid then allows the control of both the degree of condensation and oligomerization of the stabilized precursor leading to the preferential nucleation of anatase nanoparticles. We concluded that acetate acts as bidentate rather than monodentate or bridging ligand between two Ti centers. Specifically, in a 1:1 $Ti(O^iPr)_4$:CH_3COOH molar system, $Ti(OCOCH_3)(O^iPr)_2$ was determined to be the most probable species present. It was also observed that under an excess of acetic acid, the maximum coordination number of acetates is limited to 2 acetates per Ti. The synthesis route followed in this work is useful for preparing pure nanosized anatase for photocatalysis and anatase nanostructured thin films for dye-sensitized solar cells.

Acknowledgment. The authors are highly grateful to Dra. S. Santagneli for her collaboration during the NMR sessions and to Prof. J.E. Rodríguez-Páez for fruitful discussions. R.P. and M.S.G. thank FAPESP and CNPq for the postdoctoral (06/57411-9) and doctoral (141215/2006-2) fellowships, respectively. FAPESP and CNPq provided the financial support for this research.

Note Added after ASAP Publication. While this paper was in production, some important references relevant to this work were brought to the attention of the authors. The authors would like to apologize for the non-deliberate omission of these references. Prof. Sanchez et al. have previously charaterized the $Ti(O^iPr)_4$:CH_3COOH system. They have reported on the synthesis and characterization of crystallization products resulting from the modification of $Ti(O^iPr)_4$ with acetic acid. They have also proposed a mechanism for the formation of $Ti_6O_4(OCOCH_3)_4O^iPr)_{12}$ oxo-isopropoxo clusters in which acetates act mainly as bridging ligands between octahedral units. Also Prof. Birnie conducted ^{13}C NMR studies that support these structures and found that acetate modification of $Ti(O^iPr)_4$ yields a molecule of stoichiometry close to $Ti(OCOCH_3)_2(O^iPr)_2$. We suggest reading the following articles for complementary information: (1) Doeuff, S.; Henry, M.; Sanchez, C.; Livage, J. *J. Non-*

(37) Lee, G. H.; Zuo, J.-M. *J. Am. Ceram. Soc.* **2004**, *87*, 473–479.

Cryst. Solids **1987**, *89*, 206–216. (2) Barboux-Doeuff, S.; Sanchez, C. *Mater. Res. Bull.* **1994**, *29*, 1–13. (3) Stenou, N.; Robert, F.; Boubekeur, K.; Ribot, F.; Sanchez, C. *Inorg. Chim. Acta* **1998**, *279*, 144–151. (4) Birnie, D. P., III; Bendzko, N. J. *Mater. Chem. Phys.* **1999**, *59*, 26–35. (5) Birnie, D. P, III. *J. Mater Sci.* **2000**, *35*, 367–374. This paper

was originally published ASAP on November 20, 2007, and the revised version including this information was published ASAP December 12, 2007.

CM702286E